Distribution Feeder Hardening for Improving the Grid Resilience in Adverse Weather Conditions

Meher Preetam Korukonda[a], Matin Farhoumandi[a], Keith Dsouza[b], Mohammad Shahidehpour[a]
[a]Illinois Institute of Technology, Electrical and Computer Engineering Department, Chicago, IL 60616 USA
[b]Commonwealth Edison Company, Oakbrook Terrace, IL 60181 USA

***Abstract*—There has been a growing incidence of adverse weather events leading to substantial power black outs in recent years. Proper hardening of the distribution system significantly improves its resilience to extreme climatic conditions. In this paper, we propose a set of four resilience indices to evaluate the resilience of the distribution system from various perspectives and combine them into a single index to get a holistic measure of distribution feeder resilience. This resilience framework has the capability to analyze realistic performance curves (PCs) of the distribution system with multiple periods of performance degradation and recovery. Additionally, a greedy resilience hardening strategy is proposed which uses the resilience framework and historical storm outage data for determining the set of lines to be hardened to maximally improve the resilience of the distribution feeder. The proposed resilience framework and greedy line hardening strategy are implemented on a real-world distribution feeder (Feeder 91) to demonstrate their efficacy.**

***Index Terms*— Resilience planning, Line identification, Line Reinforcement, Resilience Metrics, Infrastructure Upgrade**

I. Introduction

Adverse weather events like storms and hurricanes causing extreme power disruptions to increase steadily in frequency and severity in the U.S. over the last 40 years [1]. These events result in significant economic losses, estimated between 25 to 70 billion dollars annually [2]. Historically, power system planning did not account for such extreme climate-driven disturbances. Consequently, enhancing the resilience of existing distribution systems through infrastructure reinforcements is now essential to mitigate future outages.

Providing infrastructural reinforcements in distribution systems is called hardening. Primary hardening measures like reinforcing distribution lines and properly managing vegetation are deemed to be very effective in protecting it from adverse weather events [3] and they also minimize the outages taking place due to extreme weather. However, the investment needed to carry this out successfully is substantial. Hence, designing the power system reinforcements in a cost-effective manner is a challenge on its own.

Recent studies have addressed various aspects of resilience enhancement. For instance, targeted hardening approaches that prioritize high-risk components have shown promise in improving distribution system reliability [4]. Strategic defense modeling, such as defender–attacker–defender frameworks, has also been explored in the context of both natural and malicious threats to grid infrastructure [5], [6]. These works do not consider resilience against extreme weather events.

Several recent works have further advanced the state of resilience modeling in distribution networks against extreme weather events. In [7], they propose a tri-level optimization model to select the best line reinforcements for improving resilience against storms. In [8], a data-driven spatiotemporal storm impact analysis is used to optimize resilience investment in distribution networks. [9] proposes machine-learning-guided reinforcement planning to proactively identify vulnerable feeder segments. [10] introduces a probabilistic resilience assessment framework that integrates real-time weather forecasting with outage simulation to support grid hardening decisions. Furthermore, adaptive reinforcement strategies using graph neural networks, as demonstrated in [11], offer new directions for efficiently modeling complex outage and recovery dynamics.

Recent literature [7–14] reveals two key limitations in existing resilience planning frameworks. First, many of the resilience metrics employed offer only a one-dimensional view of resilience, failing to capture its multifaceted nature. Second, these frameworks typically assume that all disruptions during extreme weather events—such as storms—occur in a single, continuous period of performance degradation, followed by a single, uninterrupted recovery phase. However, real-world storm events often exhibit more complex behavior, where some components may fail even after partial restoration has begun. This leads to performance curves (PCs) with multiple intervals of degradation and recovery, a pattern largely overlooked by current models. Additionally, most prior works do not incorporate historical outage data when assessing feeder resilience.

To address the first limitation, we previously proposed a composite resilience framework in [15] that integrates multiple performance indicators into a single index to more comprehensively quantify distribution feeder resilience. In this paper, we enhance that framework to support PCs with multiple degradation and recovery phases, aligning more closely with the realities of storm-induced outages. Furthermore, we introduce a greedy resilience enhancement strategy that utilizes both the extended framework and historical outage data to systematically identify and reinforce critical feeder lines. This approach ensures an effective balance between computational tractability and resilience improvement and is validated through case studies on a real-world distribution feeder (Feeder 91).

II. Proposed Metrics For Resilience Evaluation

PCs capture the operational performance of the feeder before, during and after adverse weather events like storms. The

This project was funded by the ComEd grant # 387574-223E-2301. The authors affiliated with Illinois Institute of Technology appreciate the support.

occurrence of extreme weather events results in outages which lead to a dip in system performance. Upon clearing the outages through appropriate restoration activities, the performance comes back to normal. The resilience evaluation framework we propose is based on the PC of the distribution feeder plotted during the storm. The performance of the feeder at any given time during the storm is described as in (1).

$$Q(t) = \frac{Total\ load\ served\ by\ the\ distribution\ feeder\ at\ time\ 't'}{Total\ load\ demand\ in\ the\ distribution\ feeder\ at\ time\ 't'} \quad (1)$$

Fig. 1. shows a typical PC of a distribution feeder with two periods of degradation and recovery. The feeder operates at a performance Q_0 at the beginning of storm t_{01}. At t_{11}, the first outage occurs, which leads to a reduction in feeder load and thus, the performance drops. Following a series of outages, the performance reaches a minimum of Q_{31} at t_{21}. Between t_{21} and t_{31}, the distribution system operators evaluate the damage done to the feeder and begin restoration of disrupted components at t_{31}. As the outages get restored, we see a gradual improvement in the feeder performance until t_{41}. However, before all the outages are recovered, new outages occur between t_{12} and t_{22} which brings about a second dip in the performance until Q_{32}. The damage is then reassessed by the operators who continue with their restoration process. At t_{42}, the performance is observed to return to pre-storm levels and at t_{52}, all the outages are restored.

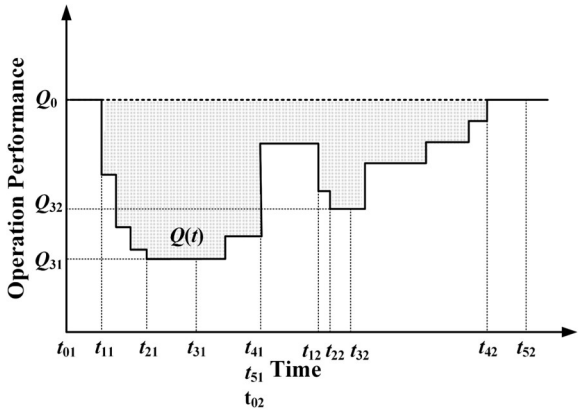

Fig. 1. PC of the feeder during adverse weather event

This PC encapsulates different resilient properties of a feeder as to how robust a feeder is towards outages or how flexible it is in responding to the outages. Hence, we propose various resilience indices based on the PC to evaluate the resilience of the feeder as shown below,

- Worst Performance (R_α): This index defined in (2) shows the least value of performance during the adverse event. It shows the retainability of power to the loads after the storm has occurred. Having a larger value of this index indicates that the feeder is more resilient.

$$R_\alpha = min(Q(t)) \quad (2)$$

- Accumulated Loss (R_β): This index shown in (3) captures the loss in feeder performance between the occurrence of first outage and restoration of last outage (i.e., between t_{11} and t_{42}). It measures the system's response to outages during the storm. Having a lower value in this index shows that the system is least affected by the adverse event.

$$R_\beta = \frac{1}{t_{42}-t_{11}} \int_{t_{11}}^{t_{42}} [1 - Q(t)]\ dt \quad (3)$$

- Resistive Capability (R_γ^k): This index shown in (4) holds an inverse relation to the rate of performance drop over a period of performance degradation. It shows how resistant a feeder is to system outages. Having a lower value of this index suggests that it degrades very quickly. In Fig. 2, there are two periods of performance degradation i.e., from t_{01} to t_{21} and another from t_{02} to t_{22}. It means that the feeder has two values of resistive capability R_γ^1 and R_γ^2. In general, the number of resistive capabilities for a specific feeder and a specific storm may be more or less depending on the PC.

$$R_\gamma^k = \frac{t_{2k}-t_{0k}}{Q_{0k}-Q_{2k}} \quad (4)$$

- Recovery Rapidity (R_δ^k): This index shown in (5) measures the speed of performance improvement over different periods of performance recovery and ranges between 0 to infinity. A larger value indicates that the system recovers swiftly from outages. There can be multiple recovery periods in the PC and the recovery rapidity is individually calculated for each period respectively.

$$R_\delta^k = \frac{Q_{5k}-Q_{3k}}{t_{5k}-t_{3k}} \quad (5)$$

- Integrated Feeder Resilience Index (R_f): The indices defined in (2)-(5) each describe a specific aspect of power system resilience. The overall definition of resilience of a feeder would be inadequate if these indices were to be used independently. We combine the previously defined indices into an Integrated Feeder Resilience Index (R_f) for describing the resilience of a distribution feeder as in (6),

$$R_f = \left[R_\alpha \,.\, (1 - R_\beta) \,.\, \prod_{k=1}^{d} \left\{ exp\left(-\varepsilon_k \,.\, \frac{1}{R_\gamma^k . R_\delta^k} \right) \right\} \right] \quad (6)$$

where ε_k is a user-specified parameter that adjusts the effect of exponential term on the index and d is the number of degradation/recovery periods in the PC.

It is reasonable to use R_f in place of multiple one-sided indices for resilience quantification. R_f ranges between 0 to 100%, in which a larger R_f denotes a higher resilience. However, every extreme event affects the feeder in a unique way and hence, an average value of the integrated feeder resilience index ($< R_f >$) computed over multiple events is used as a holistic indicator of feeder resilience.

The parameter ε governs the balance between two key dimensions of the performance curve: the magnitude of performance degradation and the duration of low-performance operation. A low ε value makes R_f highly sensitive to sharp drops in system performance, effectively highlighting scenarios where infrastructure limitations lead to severe degradation. However, in such cases, the index becomes less responsive to the length of time the system operates under degraded conditions, potentially overlooking the operational resilience aspect. Conversely, a high ε value shifts the R_f's sensitivity towards the temporal dimension, capturing extended periods of reduced performance more accurately. While this reflects the impact of operational strategies in an enhanced manner, it can underrepresent the severity of performance drops.

The optimal choice of ε should reflect the nature of the loads connected to the feeder. For feeders supplying critical loads like hospitals—where sustained low performance is preferable to complete outages—a lower ε

emphasizes the importance of maintaining any level of service. In contrast, feeders serving facilities like airports—where quick restoration is essential even if temporary outages occur—benefit from a higher ε, which prioritizes timely recovery over immediate performance dips. In essence, ε serves as a tuning knob that aligns the R_f with the resilience priorities of different types of electrical loads, making careful selection essential for meaningful resilience assessment.

III. Proposed Hardening Strategy

The idea of the line hardening strategy is to find the best set of lines to be reinforced in the distribution feeder so as to maximize the feeder's resilience to extreme weather events. The flowchart for the greedy line reinforcement strategy is shown in Fig. 2.

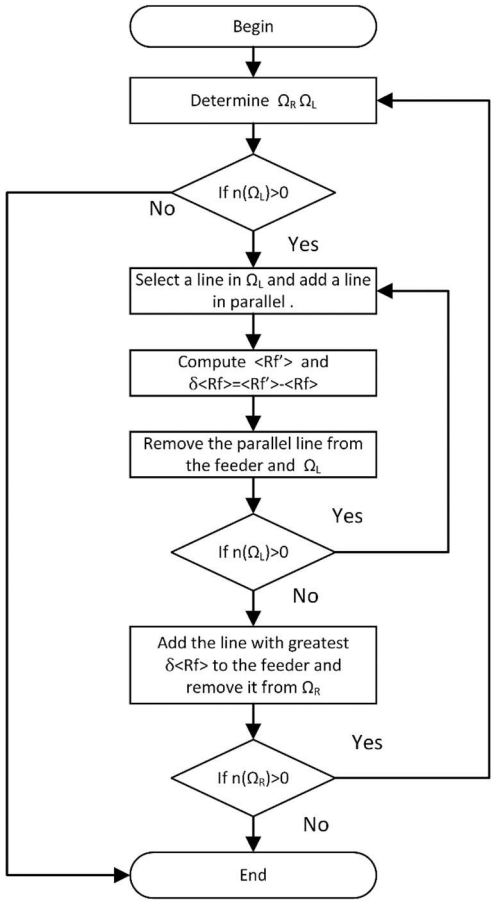

Fig. 2. Flowchart for the Greedy Line Reinforcement Procedure

The first step in this process is to determine Ω_L and Ω_R. Ω_R is the set of planned line reinforcements and Ω_L is the set of identified lines for reinforcement testing. Ω_R is decided by investors based on budget. To populate Ω_L, we look for two types of lines, namely, the lines along which outages occur and the lines that get loaded to maximum capacity during storms. The lines along which the outages occur are determined from historical data whereas the lines that get loaded to maximum capacity are determined after running the power flow analysis for various historical storms.

Following this, we select a line in Ω_L, provide reinforcements to the selected line and run the power flow for various historical storm outage data. The new average feeder resilience $< R_f' >$ and improvement in average feeder resilience $< \delta R_f > = < R_f' > - < R_f >$ is computed after adding the new line. This process is repeated for all the lines in Ω_L. The line with the highest value of $< \delta R_f >$ is selected and added to the distribution feeder. Once, the line is added to the feeder, it is deleted from Ω_L.

If there are more lines to be reinforced or Ω_R is non-empty, we repopulate Ω_L and repeat the process. This procedure continues till all the planned lines are reinforced at suitable locations.

IV. Results and Discussion

A. *Average Feeder Resilience($< R_f >$) Evaluation:*

Fig. 3. shows the one-line diagram of a three-phase unbalanced distribution system called Feeder 91. Feeder 91 contains a total of 91 nodes and 91 lines with the substation located at 903. The feeder operates at a base voltage of 12.5 kV and serves a load demand of 6.42 MW and 3.05 MVAR.

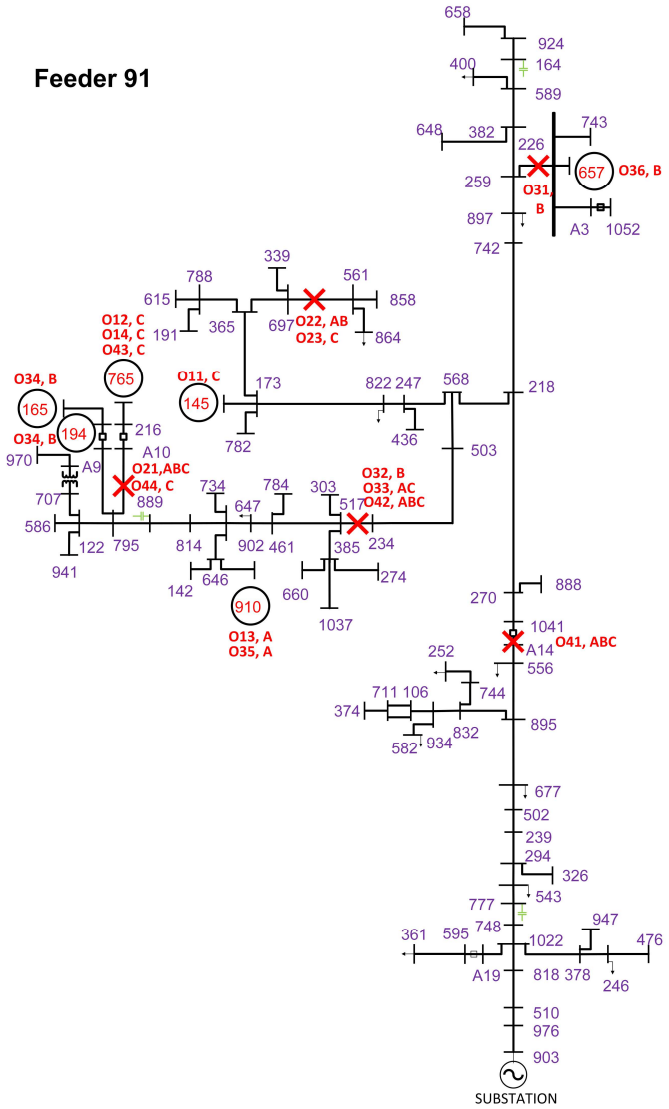

Fig. 3. One line diagram of Feeder 91 with all the outages of four storms

To evaluate the average feeder resilience index for Feeder 91, we use the outage data related to four different storms namely Storm 2017, Storm 2019, Storm 2021, and Storm 2022 that affected the feeder in the past. Table I provides the information on these outages including location of the outage, time of outage and time of recovery during all the historical storms. O11-14 belong to Storm 2017, O21-23 belong to Storm 2021, O31-36 belong to Storm 2019 and O41-44 belong to Storm 2022. All these outages are marked in red in Fig. 3.

The outages in these cases can be classified into two types – outages at specific nodes and outages along the line. When outages occur at a specific node, they disconnect the loads present only at a particular node. However, when outages occur along a line, they result in disconnecting more loads connected to other nodes along the line on outage. The outages affecting specific nodes are marked in Fig. 3. By a black circle with the node number written in red and the outages along the line are marked with a red cross on the line. The outage names along with the phases affected by the outage are also marked in red.

1) Case 1: Storms with outages on specific nodes

In the case of Storm 2017, the four outages O11-O14 shown in Table I disconnect loads at specific nodes. Such outages result in smaller performance dips compared to the outages along the line. The PC for Feeder 91 is plotted after running the power flow analysis on an hourly basis as outages occur and get repaired during the storm and is shown in red in Fig. 4.

TABLE I
OUTAGE DETAILS FOR THE FOUR STORMS

Outage Name	Outage Time(hr)	Recovery Time (hr)	Outage Name	Outage Time (hr)	Recovery Time (hr)
O11	3	32	O33	6	10
O12	3	35	O34	11	15
O13	21	26	O35	11	22
O14	33	35	O36	15	26
O21	2	18	O41	4	20
O22	16	48	O42	18	19
O23	47	48	O43	20	24
O31	4	12	O44	23	24
O32	5	10			

At the beginning of the storm, all the loads in the feeder are connected to the substation at 903. Since all the loads are connected, the performance of the feeder is initially at 1. At t=3, outages O11 and O12 occur which disconnect 8.25kW load on the C phase of node 145 and 10.32 kW on the C phase of node 765. Due to this, a drop in performance is observed. At t=21, outage O13 disconnects 18kW on phase A at node 910 which further drops the performance. The loads disconnected due to outage O13 get re-connected to the feeder at t=26 and increase the performance. Following this, the outage O11 gets restored at t=32 leading to further increase in the system performance to 0.998. However, before recovering from all the outages, another outage occurs at t=33 in which 110kW load was disconnected leading to a steep decline in the system performance. Following this, O12 and O14 are repaired immediately at t= 35 and the system returns to pre-storm performance levels.

In the red colored PC shown in Fig. 4, there are two periods of performance degradation, one from t=0 to t=21 and t=32 to t=33. Similarly, there are also two periods of performance recovery, one from t=23 to t=32 and another from t=33 to t=35. While the worst performance (R_α) and the accumulated loss (R_β) are computed for the entire PC, the resistive capability (R_γ^k) and recovery rapidity (R_δ^k) are computed individually for the two respective periods of degradation and recovery. The integrated feeder resilience index (R_f) is finally computed using (6). All the computed resilience indices for this case are shown in Table II.

2) Case 2: Storms with outages along the line

The details of Storm 2021 are provided in Table I. In this storm, there are three outages O21-O23 that happen along the line. The associated PC is plotted in red in Fig. 5.

The first outage O21 occurs at t=3 due to opening of the line recloser between 795 and 216. Since the line recloser is situated between the two nodes, when it opens, it disconnects all the loads present on both 216 and 765 which is beyond 216. Node 795 is still connected to the substation. The performance of the feeder reduces from 1 to 0.965.

It further reduces when O22 happens and the fuse between 561 and 697 opens at t=16 and disconnects the loads on 561, 858 and 864. This is followed by O23 at t=47 leading to a minor dip in performance followed by recovery of O22 and O23 at t=48 leading to full feeder recovery. The computed resilience indices are shown in Table II.

TABLE II
RESILIENCE INDICES FOR THE FOUR STORMS

Case	R_α	R_β	R_γ^1	R_γ^2	R_δ^1	R_δ^2	R_f (%)
1	0.9828	0.0049	3230.76	135.135	0.00045	0.008	87.5
3	0.6553	0.0809	17.4064	57.8035	0.1094	0.003	44.3
2	0.9465	0.0251	299.101	3670.04	0.0177	0.026	90.5
4	0.1917	0.6486	4.9489	135.197	0.0895	0.032	5.32

3) Cases 3-4: Storms with mixed outages

In cases 3 and 4, we subject Feeder 91 to Storm 2019 and Storm 2022 with mixed outages, i.e., some outages happen along a line and some outages are limited to only specific nodes. as shown in Fig. 3 and Table I. The PCs for both these storms are shown in Fig. 6. and Fig. 7, in red, and the computed resilience indices for these two cases are shown in Table II.

B. Resilience based Line Reinforcement Strategy

In the previous subsection, the $< R_f >$ of Feeder 91 is evaluated as 56.92% and thus needs to be enhanced. The location where a line is placed has an important role in determining the resilience enhancement of the feeder. For instance, if a new line is placed in parallel to a line which is never affected by any storm, the new line would not contribute to preserving any additional loads during outage and thus, it would not improve the resilience of the feeder. However, reinforcing lines that get frequently overloaded would improve power delivery to additional loads in the feeder during outages leading to better feeder resilience.

In this paper, the objective is to select two lines for reinforcement among the 91 lines in Feeder 91 that enhance its resilience to the maximum. Hence, Ω_R contains two lines L1 and L2. According to the algorithm, we find the set of outages that lead to disconnection along the line from the available outage history on the four storms. The lines along which the outage occurs are marked and populated into the set Ω_L. We further check for any lines which were overloaded during the

four storms and add them to Ω_L. The various lines present in Ω_L and their associated $< \delta R_f >$ values after reinforcing the original feeder are shown in Table III. We choose to place line L1 between 556 and 1041 as it contributes to the highest improvement in average feeder resilience (14.19%).

TABLE III
$< \delta R_f >$ COMPUTATION FOR CHOOSING THE LOCATION OF L1

Elements in Ω_L	From Node	To Node	$< R_f >$	$< R'_f >$	$< \delta R_f >$
1	259	226	71.11	70.4	-0.71
2	234	517	71.11	88.71	17.6
3	795	216	71.11	72.35	1.24
4	697	561	71.11	63.31	-7.8

According to the algorithm, after the first line L_1 is placed between 556 and 1041, it gets deleted from Ω_L and Ω_R. However, Ω_R is still not empty. Hence, after adding the first line reinforcement, we rerun the power flow for all the four different storms and repopulate Ω_L. The new elements in Ω_L and the associated $< \delta R_f >$ are shown in Table IV. The best location for adding line L_2 is between nodes 234 and 517 since it improves the average feeder resilience by a further 17.6%. It can be seen in Table III and Table IV that when some lines are reinforced, the resilience decreases. This is because, when some lines are reinforced, the time of degradation gets greatly reduced leading to very low resistive capability values that reduce the overall resilience of the feeder.

TABLE IV
$< \delta R_f >$ COMPUTATION FOR CHOOSING THE LOCATION OF L2

Elements in Ω_L	From Node	To Node	$< R_f >$	$< R'_f >$	$< \delta R_f >$
1	259	226	56.92	56.71	-0.21
2	234	517	56.92	66.19	9.27
3	795	216	56.92	58.1425	1.2225
4	697	561	56.92	49.1225	-7.7975
5	556	1041	56.92	71.11	14.19

The total number of combinations of the locations we had to check was only 5+4=9 instead of 8281 (91x91) if we used brute force. This shows that the greedy hardening strategy gives us great computational advantage over the brute force method. The PCs for the four storms after adding the reinforcements L_1 and L_2 are shown in blue in Fig. 4. to Fig. 7.

In Fig. 4. and Fig. 5, we see that there is no improvement in the PC even after adding L_1 and L_2. This is because all the outages in Case-1 occur directly at the node and adding a new line nearby does not provide for disconnected loads. In Case-2, the added lines do not provide any alternate paths for the electricity to provide extra loads and hence, the PC doesn't change. In the remaining two cases, the outages that take place along the lines are reinforced. The load loss due to this type of outage is mitigated when redundant lines are present in the vicinity of outage and hence the performance improves. This is reflected in Fig. 6. and Fig. 7. The average resilience of the feeder is seen to improve from 56.92% to 88.71%.

Although this reinforcement selection technique is fast and easy to implement, it has some limitations. The algorithm is based on greedy strategy which has the tendency to produce suboptimal solutions, as it makes decisions based solely on immediate gain without considering the global context. It does not have the facility to backtrack or revise previous choices, making it inflexible if an early decision is incorrect. In general, greedy algorithms lack the exhaustive search capability needed to explore all possible solutions. As a result, they cannot guarantee optimality in most scenarios.

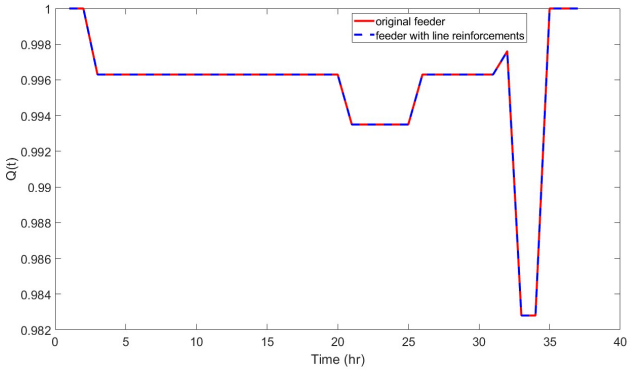

Fig. 4. PC for Feeder 91 during Storm 2017 before and after L_1 and L_2.

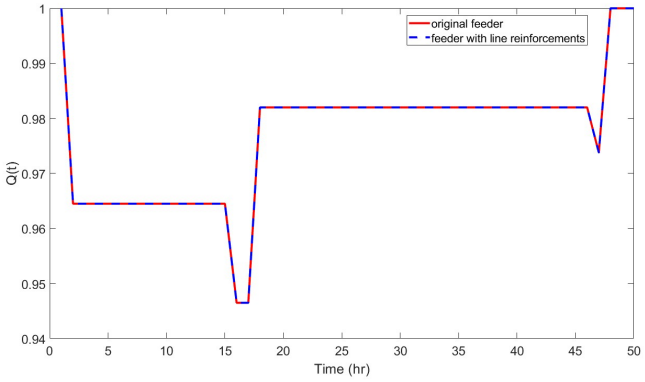

Fig. 5. PC for Feeder 91 during Storm 2021 before and after L_1 and L_2.

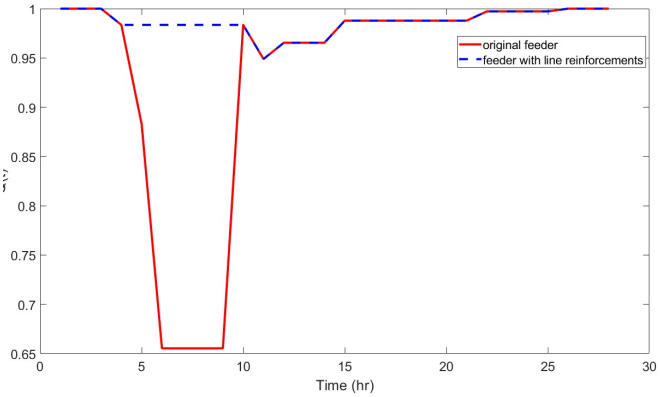

Fig. 6. PC for Feeder 91 during Storm 2019 before and after L_1 and L_2.

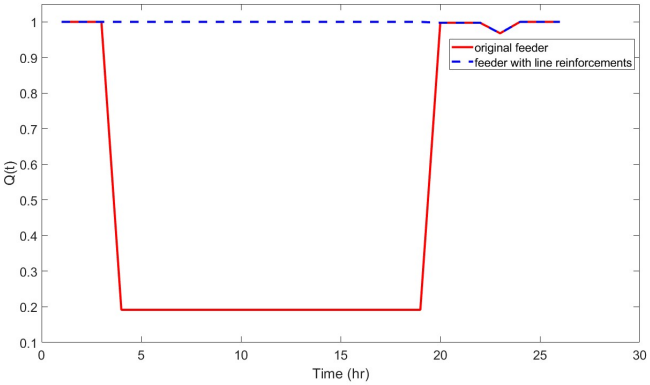

Fig. 7. PC for Feeder 91 during Storm 2022 before and after L_1 and L_2.

V. Conclusion

In this paper, we proposed various indices for evaluating the resilience of distribution feeders with historical outage data having PCs with multiple periods of performance degradation and recovery. The resilience framework and the greedy line hardening strategy is successfully tested on a 91-bus feeder. The conducted studies found that the proposed resilience analysis framework clearly reflects the resilience of the distribution feeder both in the presence and in the absence of reinforcements. The proposed greedy strategy greatly reduces computational complexity in the process of finding the lines to be reinforced to get maximum increase in feeder resilience.

Implementing the proposed resilience framework and greedy reinforcement strategy in real-world settings faces several practical challenges. Key among these is the limited availability and quality of detailed historical outage and load data, which are essential for accurate performance curve analysis. Although the greedy algorithm reduces computational burden compared to brute-force methods, it still requires significant processing power, especially for large or complex feeders. Additionally, the method's adaptability to diverse feeder types and operational conditions may require customization, potentially limiting its generalizability across different utility networks.

In the future, along with the historical data, we will also employ a probabilistic framework to incorporate more adverse events for evaluating the feeder resilience. This will help us to reduce our reliance on accurate historical data. We will also extend the greedy framework to determine the best mix of resilience enhancement options including pole upgradation, line reinforcement, DG placement, etc within a given budget.

References

[1] A. B. Smith, "U.S. Billion-Dollar Weather and Climate Disasters 1980—Present," NOAA National Centers for Environmental Information, Jun. 2020, [online] Available: https://doi.org/10.25921/stkw-7w73.

[2] "Electricity and grid resilience: Climate change is expected to have far-reaching effects and DOE and FERC should take actions," Washington, DC, USA, United States Government Accountability Office (GAO), 2021.

[3] Z. Yu, G. Zou, L. Wu, J. Zhang, and Z. Li, "Optimal Resilience Enhancement Strategy for Power Distribution System with Line Reinforcement and Emergency Generator Placement," 2021 IEEE Sustainable Power and Energy Conference (iSPEC), Nanjing, China, 2021, pp. 1400-1405, doi: 10.1109/iSPEC53008.2021.9735857.

[4] A. M. Salman, Y. Li, and M. G. Stewart. "Evaluating system reliability and targeted hardening strategies of power distribution systems subjected to hurricanes," Reliab. Eng. Syst. Saf., vol. 144, pp. 319-333, Jul. 2015.

[5] Natalia Alguacil, Andrés Delgadillo, José M. Arroyo, "A trilevel programming approach for electric grid defense planning," Computers & Operations Research, vol. 41, 2014, pp. 282-290, ISSN 0305-0548, https://doi.org/10.1016/j.cor.2013.06.009.

[6] Wei Yuan, Long Zhao, Bo Zeng, "Optimal power grid protection through a defender–attacker–defender model," Reliab. Eng. Syst Saf, vol. 121, 2014,pp.83-89,ISSN0951-8320, https://doi.org/10.1016/j.ress.2013.08.003.

[7] Y. Tan, A. K. Das, P. Arabshahi and D. S. Kirschen, "Distribution Systems Hardening Against Natural Disasters," in IEEE Transactions on Power Systems, vol. 33, no. 6, pp. 6849-6860, Nov. 2018, doi: 10.1109/TPWRS.2018.2836391.

[8] J. Liu, M. Kezunovic, and Y. Ding, "Spatiotemporal Storm Impact Analysis for Optimal Resilience Investments in Distribution Grids," IEEE Transactions on Smart Grid, vol. 15, no. 1, pp. 341–352, Jan. 2024. doi: 10.1109/TSG.2023.3319847.

[9] H. Park, R. Arghandeh, and M. S. Brown, "Machine Learning-Guided Resilience Planning in Electric Distribution Networks," IEEE Transactions on Power Systems, vol. 39, no. 2, pp. 1150–1161, Mar. 2024. doi: 10.1109/TPWRS.2023.3324050.

[10] Y. Zhang, S. Dey, and P. K. Sen, "Probabilistic Framework for Resilience Evaluation under Dynamic Weather Conditions," IEEE Access, vol. 12, pp. 21840–21853, 2024. doi: 10.1109/ACCESS.2024.3351124.

[11] L. Chen and X. Zhang, "Adaptive Power Grid Reinforcement Using Graph Neural Networks," 2024 IEEE PES General Meeting (PESGM), Seattle, WA, 2024, pp. 1–6. doi: 10.1109/PESGM57950.2024.10345678.

[12] S. Espinoza, M. Panteli, P. Mancarella, and H. Rudnick, "Multi-phase assessment and adaptation of power systems resilience to natural hazards," in Electric Power System Research, vol. 136, pp. 352–361, Jul. 2016.

[13] M. Panteli, P. Mancarella, D. N. Trakas, E. Kyriakides and N. D. Hatziargyriou, "Metrics and Quantification of Operational and Infrastructure Resilience in Power Systems," in IEEE Transactions on Power Systems, vol. 32, no. 6, pp. 4732-4742, Nov. 2017.

[14] D. A. Reed, K. C. Kapur and R. D. Christie, "Methodology for Assessing the Resilience of Networked Infrastructure," in IEEE Systems Journal, vol. 3, no. 2, pp. 174-180, June 2009, doi: 10.1109/JSYST.2009.2017396.

[15] M. P. Korukonda, S. Pandey, H. Zheng, A. Alabdulwahab, A. Abusorrah and M. Shahidehpour, "A Quantitative Framework to Evaluate the Resilience Enhancement in Power Distribution Feeders During Adverse Weather Events," 2023 5th Global Power, Energy and Communication Conference (GPECOM), Nevsehir, Turkiye, 2023, pp. 425-430, doi: 10.1109/GPECOM58364.2023.10175669.